ADVANCES IN MATERIAL STUDIES FOR SRF*

T.R. Bieler#, Michigan State University, East Lansing, MI 48824-1226 U.S.A.

Abstract

In the past decade, high Q values have been achieved in high purity Nb superconducting radio frequency (SRF) cavities. Fundamental understanding of the physical metallurgy of Nb that enables these achievements is beginning to reveal what challenges remain to establish reproducible and cost-effective production of high performance SRF cavities. Recent studies of dislocation substructure development and effects of recrystallization arising from welding and heat treatments and their correlations with cavity performance are considered. With better fundamental understanding of the effects of dislocation substructure evolution and recrystallization on electron and phonon conduction, as well as the interior and surface states, it will be possible to design optimal processing paths for cost-effective performance using approaches such as hydroforming, which minimizes or eliminates welds in a cavity.

INTRODUCTION

The continuing efforts to improve cavity performance to attain a high electric field and quality (efficiency) factor, Q, have shown that the theoretical limit for the maximum field of about 42 MV/m is within reach [1]. As this limit is approached, identification of factors accounting for sub-theoretical performance becomes increasingly important in order to reduce variability in performance. A number of hypothetical reasons have been put forward, many of which are linked to the metallurgical state of the Nb, particularly in welds. As there are many possible variables, discussion will become less speculative if fundamental understanding of the physical metallurgy processes that occur along the fabrication path are clarified. This paper provides an overview of what is known about the evolution of metallurgical state, and identifies areas needing further examination.

The primary focus will be on factors that affect formability of Nb and cavity performance based upon classical [2-4] mechanical and physical metallurgical knowledge. These topics are insufficient to identify what accounts for variability in performance, as there are additional factors related to electromagnetic and superconducting states in the few nanometers near the surface of the interior, which are discussed in other papers [5-7]. This paper will focus on the evolution of defect structures, primarily dislocation substructure, and how it affects cavity manufacturing and performance. Thus, the basic crystal structure is discussed first, followed by physical metallurgical changes that occur with forming, welding, heat-treating, etching and baking.

BCC DISLOCATION CHARACTERISTICS

Pure Nb is a BCC (body centered cubic) metal similar to steel in structure only, as steels contain other elements (always C, S, P, Mn, sometimes Al, Si, Ti, V, Cr, Ni, Nb, Mo). Much of the metallurgy of steel is focused on exploiting the phase transformation from FCC (face centered cubic) to BCC (Figure 1) that occurs around 700-900 °C, and controlling the distribution of C in interstitial positions and carbide precipitates. Interstitial carbon and small precipitates have a large influence on generation of mobile defects such as vacancies and dislocations (terminated half-planes), which determine strength and ductility of the alloy. In FCC metals (e.g. Al, Cu, some stainless steels), dislocation and mechanical twinning processes are confined to {111} planes with dislocation motion in the <110> and <112> twinning directions†. Conversely, dislocations in the BCC structure move in <111> directions on {110}, {112}, and {123} planes. In FCC metals, there are 12 slip systems of 3 slip directions on 4 slip planes. In BCC metals, there are 6 {110} slip planes on which there are 2 slip directions giving 12 slip systems. Because BCC metals are also able to slip on {112}, and {123} planes in the 4 <111> directions, BCC metals have 48 slip systems available. There are 2 equivalent descriptions for each system, as illustrated in Figure 2, where each slip systems is defined with a plane and shear direction. Operation of several slip systems are usually required to change shape, leading to complex intersections and entanglements.

In the BCC structure, dislocations reside in deep energy wells, and their motion requires significantly greater mechanical force than in FCC metals, but thermal vibration provides a large fraction of the energy needed to move dislocations. This makes all BCC metals very

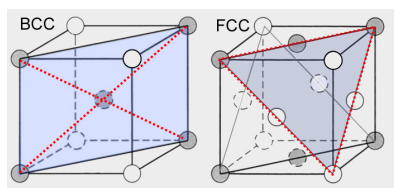

Figure 1: Comparison between BCC and FCC crystal structures. Examples of slip planes are shaded, and slip directions identified with red dotted lines.

* This work has been funded by research contracts from DOE (ILC, SBIR), and Fermi National Laboratory, and represents work done by graduate students D. Baars, A. Zamiri, H. Jiang, S. Chandrasekaran, S. Balachandran and advisors N.T. Wright, F. Pourboghrat, at MSU, C. Compton at the National Superconducting Cyclotron Laboratory, and K.T. Hartwig at Texas A&M University and Shear Form, Inc.

bieler@egr.msu.edu

† The symbols { } and < > around 'Miller indices' are used to describe families of similar (symmetric) crystallographic planes and directions, respectively, in terms of the cubic lattice. The symbols ( ) and [ ] refer to specific members of the family of planes and directions, respectively, arising from any permutation of positive and negative integers in the family. For example, 4 <111> directions, 6 {110} planes, 12 {112} planes, and 24 {123} planes are present in any cubic structure.

strong at cryogenic temperatures. The yield stress in BCC metals is also highly sensitive to the interstitial atom content, as interstitial atoms will diffuse into dislocation cores even at room temperature. These interstitials raise the mechanical energy needed to force dislocations to break away from the solute atoms that pin them, leading to an initial yield drop when the stress is sufficiently high, as is observed in lower purity Nb. Because of the temperature range of the FCC-BCC transformation in steels, and the high rate of atom diffusion at those temperatures, the range of microstructures and properties that can be obtained in steels is extensive.

Pure Nb has none of the complication of steels, and in contrast to Fe, only the grain size and dislocation substructure can be modified. Furthermore, the elastic anisotropy of Nb is the opposite of Fe, as illustrated in Figure 3 [8], which affects the characteristics of dislocations in Fe and Nb. In Fe, the direction of <111> dislocation slip is in the stiffest direction in the crystal, whereas in Nb, it is the most compliant (Nb is the most compliant of all the BCC metals, which may arise from Nb being the only Group 5 metal with an extra d shell electron instead of a filled s shell).

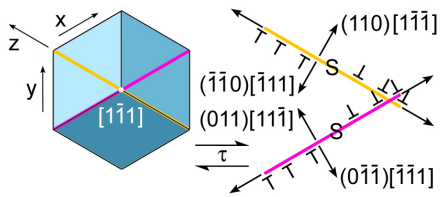

Figure 2: Schematic diagram of motion of dislocations from sources S due to an imposed shear stress τ that activates two slip systems. The plane normal and direction of motion are described with Miller indices such that the scalar produce is zero; each system can be equivalently described in two ways using opposite signs (bars over numbers).

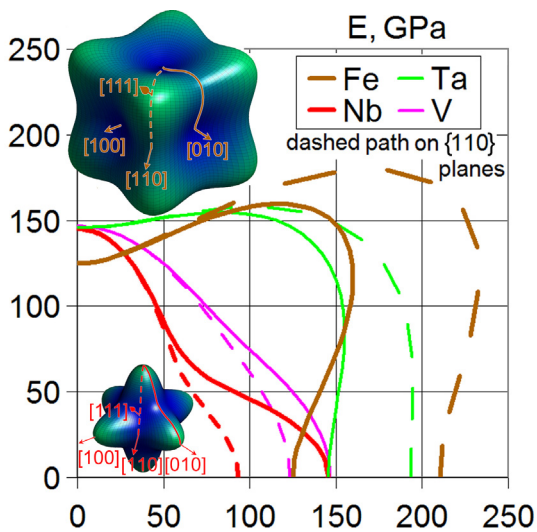

Figure 3: The elastic anisotropy of BCC metals is plotted on {100} and {110} planes showing maximum and minimum values of Young's (tensile) modulus, E (the vector from the origin to the curve gives the direction and magnitude). The maximum stiffness in Fe is <111>, which the most compliant in Nb. Nb is the most compliant of BCC metals [7].

As dislocations on a slip plane impose an elastic repulsive force on neighboring dislocations, a pileup of dislocations generated by strain against a grain boundary (which controls the yield stress) leads to internal elastic back stresses that resist formation of more dislocations. The stress imposed on a barrier (such as a grain boundary or an entanglement) by a pileup of dislocations is proportional to $n\tau$, where n is the number of dislocations in a pileup and τ is the stress needed to initiate slip. Consequently, to achieve the same internal stress in Nb as in Fe, Nb would require more than 3 times the number of dislocations, as $E_{111}(Fe)/E_{111}(Nb) = 3.3$. Because the interaction forces between dislocations in Nb are much smaller, dislocation entanglements lead to much smaller internal stresses in Nb, and hence are much more stable.

Figure 4 shows stress-strain curves for nine single crystal orientations [9]. Experiments conducted in the 3-D diffraction microscope at the Advanced Photon Source (APL) at Argonne National Laboratory reveal information about dislocation substructure. In specimens with much work hardening, diffraction patterns show streaked spots, whereas nearly perfect spots are observed in specimens oriented for single slip on a facile slip system. The streaks indicate the presence of orientation gradients, and by implication, dislocation entanglements. In contrast, where slip occurred without entanglements, dislocations were able to enter and leave the crystal without causing any orientation gradients, resulting in only a small amount of hardening (stress increase). Dislocation motion in BCC metals is complex, as indicated by 4 of the 9 samples exhibiting flow softening (stress decreases after a peak stress), which may depend on orientation softening, or complex dislocation behavior proposed by other researchers [10-11].

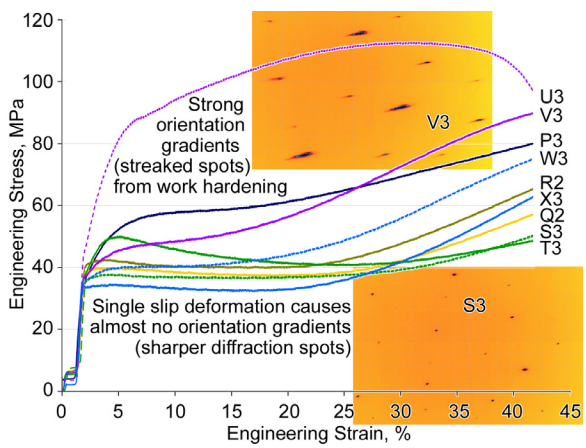

Figure 4: Stress strain curves for 9 single crystals oriented to investigate slip system operation; some have single slip for much of the deformation (flat curves), 4 show softening (R2,X3,Q2,T3), and others have multiple slip systems activated that cause stress increases (work hardening) from dislocation intersections and entanglements.

INGOT PRODUCTION

As high purity Nb is produced using multiple electron beam remelts of a Nb ingot, the solidified lower part of the ingot collects droplets of molten Nb, and hence the top of the ingot is at the melting temperature. The water cooled mold causes a large spatial temperature gradient, yet the cooling rate is slow. These conditions favor growth of large grains due to the slow cooling rate, but the large temperature gradient also causes strains associated with thermal contraction. Figure 5 shows a region in a large grain ingot with significant populations of tangled dislocations (white) that are between cells of low dislocation density material (dark) [12]. It is yet unclear if this heterogeneous dislocation structure is typical, but such dislocation structures cause several degrees of orientation spread within a grain, which has been observed consistently in inverse pole figures obtained from orientation imaging microscopy (OIM) data sets (Figure 6). This orientation spread implies that there are more geometrically necessary dislocations than are observed in recrystallized grains (discussed later).

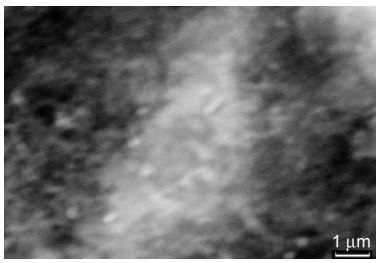

Figure 5: Electron Channelling Contrast Image of dislocation structure in an as-received ingot.

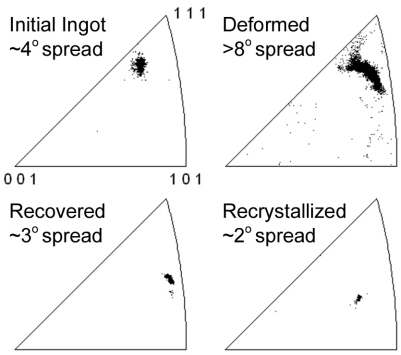

Figure 6: Representative discrete inverse pole figures from OIM measurements. The spread of crystal orientations is greatest after deformation, and significantly lower after heat treatments to cause recovery or recrystallization.

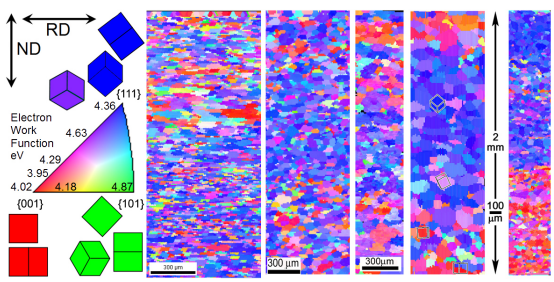

Figure 7: Five examples of orientation maps from commercially rolled high Purity Nb show a trend of preferred {100} orientations near the surface and {111} orientations in the interior. Microstructure and texture gradients vary widely from sample to sample. The orientation maps are with respect to the sheet normal direction, and electron work function values are indicated for different surface normal directions.

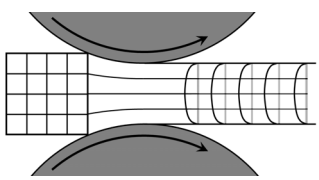

Figure 8: Schematic diagram illustrating how the strain path differs between the surface and center of rolled sheet. The relative amount of shear at the sheet is increased with smaller reductions.

SHEET METAL PRODUCTION

Rolling accomplishes two goals, to break down the initially large grains to create a uniform fine grain size, and to change the shape into sheet metal. Ingots are sectioned into billets (which may only contain a few grain orientations) and cold forged to a suitable shape that is then rolled using multiple reductions according to typically proprietary schedules, and annealed at strategic times during this process [13]. As high purity Nb is not a mass produced product, the billet is commonly small enough to allow rolling in multiple directions, which can improve the uniformity of the properties of a rolled sheet.

The rolling process commonly causes activation of slip systems that rotate crystals in the center of the sheet so that {111} is approximately parallel to the sheet normal direction (ND), and grains on the surface to have {100} parallel to the ND, as illustrated in Figure 7. The difference between the surface and interior orientation arises from an extension strain path in the center and a shear-dominated strain path on the surface layer (due to the effects of the rolls, see Figure 8 [4]). Because these two strain paths have different stress states, they cause different rotations and different levels of stored strain energy (dislocation density), so recrystallization is rarely uniform. Often, the surface shows larger grain sizes than in the interior. To achieve a sufficiently uniform small grain size (to meet specifications), producers have often given a small reduction prior to the final anneal that selectively puts more plastic work into the surface grains. While this leads to a more consistent grain size, it also increases the fraction of {100} grains on the surface.

A common orientation found on the surface is the {100}<011>* rotated cube orientation. More commonly,

* The {plane}<direction> nomenclature identifies an orientation about which there is commonly a spread of about 10°. {100}<011> indicates that {100} planes are approximately parallel to the sheet (i.e. the plane normal is perpendicular), and <011> directions are aligned preferentially with the rolling direction (RD). It is usually written so that the scalar product would be zero, consistent with the orthogonal relationship between the sheet normal and the rolling direction.

a range of orientations with a common plane normal direction, such that {100} ‖ ND describes an axis about which any rotation of the crystal about the sheet normal direction can be found. Similarly, a {111} ‖ ND preferred orientation is also commonly found (named the γ fiber), and this orientation is very desirable for uniform forming characteristics.

From about 10 characterizations of different batches of rolled material from different suppliers, the same combination of texture and grain size has never been observed twice, even among pieces from the same batch of material. One of the examples in Figure 7 even shows the upper half with {100} and the lower half with {111} planes preferred in the sheet normal direction. This implies that a method to reproduceably obtain the same microstructure from a billet has not been achieved, and this can cause variability in forming half-cells.

Some of the variability in cavity performance may be traceable to the variability of grain orientations on the surface, which etch at different rates, and have different work functions (the work function varies with surface normal direction as illustrated in Figure 7).

INFLUENCE OF MICROSTRUCTURES ON FORMABILITY

Processes have been developed to optimize uniform in-plane formability of steel sheets by controlling texture and microstructure. It is well established that a small grain size favors more uniform and larger strains, and also minimizes surface roughness (orange-peel) that arises from heterogeneous strain in different grains. Minimizing surface roughness minimizes perturbations that can initiate fatigue cracks, and as important, improve the application and appearance of paint.

Texture is controlled by strategic deformation and heat treatment sequences. The {100} ‖ ND is an undesirable soft, but stable orientation, as the operation of several slip systems lead to localized oscillating counter-rotations that maintain the same crystal orientation. For example the rotated cube orientation is stable up to 70% thickness reduction, after which slip commences on {123} planes that alters the orientation [14]. In the {100} ‖ ND orientations, all four <111> slip directions have a ~35° inclination from the sheet that causes high resolved shear stresses on many slip systems. This orientation causes the greatest tendency for thinning in the sheet with strain, which creates local thin spots that cause a self-amplifying strain localizing effect. In contrast, the {111} ‖ ND orientation has 3 <111> directions inclined 20° from the plane, and the 4th one is perpendicular (and has a near-zero resolved shear stress acting on it). Because of the small angle, a large applied stress is needed to reach the yield stress, making it a hard orientation. This is also a stable orientation because if two slip systems operate preferentially, they will rotate the crystal in a direction where the third one becomes favored, causing a counter rotation. With the small inclination of slip direction from the sheet plane, this orientation resists thinning. When there is a high volume fraction and a uniform distribution of orientations around the γ fiber, very uniform deformation and large strains are enabled, so great effort is taken to make this the dominant texture component. Other orientations are not stable; when slip occurs predominantly along one or two <111> directions, the crystal must rotate. As Figure 7 shows a variety of orientations present on the surface, the rate of thinning varies from grain to grain, which causes the 'orange peel' effect on the surface. Hence, minimizing the red and maximizing the blue orientations will also improve the surface uniformity, stable deformation, and reproducibility of strains.

With increasing strain, the crystals rotate toward either the {100} ‖ ND or {111} ‖ ND orientations, but only the {111} is desirable. Strategic changes in rolling direction combined with heat treatment can bias the rotations toward a desired orientation, but when the final thickness is reached, strain can no longer be used to change the texture. This limitation on the available strain can be overcome to obtain highly desirable textures with fine grain sizes using the Equal Channel Angle Extrusion processes prior to rolling, as indicated in Figure 9 [15]. A billet of material is pushed through the 90° die several times without changing the shape, so with different sequences of rotations, very different textures and microstructures can be obtained. After this strategic preconditioning that homogeneously generates a fine grain size and a more uniform texture, subsequent rolling can lead to more reproducible microstructure and texture, and hence formability (and hence, less variability).

Computational plasticity modeling strategies can be used to simulate these processes, and to use optimization methods to identify desirable processing strategies. Using the measured texture as an input, these orientations can be computationally deformed in a manner that insures compatibility in strains (so that no voids occur) on an average (statistical) basis, or, as simulations of particular microstructures. With different combinations of slip systems active in each grain, the amount of slip on each system varies *within* grains so that compatible deformation occurs with neighboring grains. These modeling processes are complex, and must consider how accumulation of dislocations hardens the microstructure and increases the stress needed to accomplish the next increment of deformation, and hence, rotation. Figure 10 shows two outcomes starting with the same set of grain orientations, but using different ways of tracking hardening behavior; the more sophisticated model is able to predict locations where failure is more likely [16].

Slicing Ingots to form Cavities

There is growing interest in bypassing the cost and uncertainties associated with rolled material by slicing ingots and forming cavities from the multi- (or sometimes single-) crystal slices from ingots [13]. When pressed in molds, the deformation is often much more irregular than from fine grain sheet metal, requiring extra pressing operations and jigs to obtain circular mating surfaces

needed to weld two half cells together. Thicknesses are much more irregular, even within the same grain orientation, because the direction of hoop stress varies spatially with respect to the grain orientation, such that different slip systems will be activated in different parts of the same large grain. Grain boundaries impose barriers to slip, so that less strain occurs along grain boundaries, leading to easily detected ridges along grain boundaries. These irregularities may be worth tolerating for benefits that come with reduced waste material and reduced cost from rolling and heat treating, but this also introduces an element of variability that must be either tolerated or overcome with strategic processing of ingots to obtain consistent grain orientations, or strategic choices of which pieces (and orientations) should be welded together.

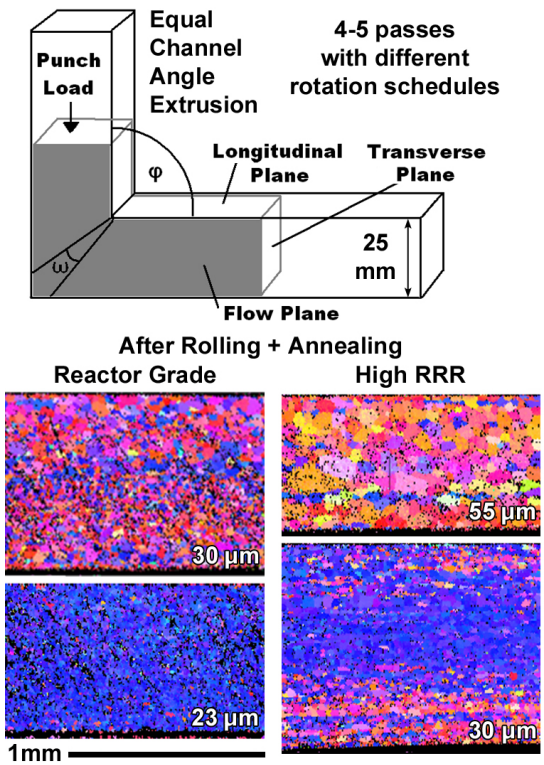

Figure 9: Very different kinds of rolled sheet microstructures and texture gradients can be obtained for samples preprocessed with ECAE; the color scale is the same as Figure 7.

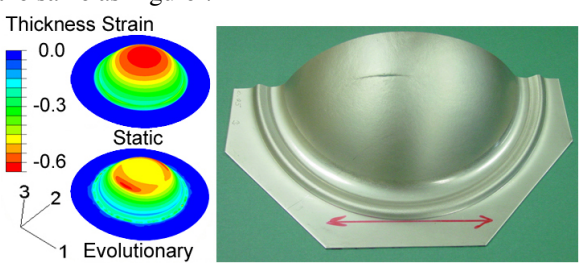

Figure 10: Simulations of biaxial bulging using two variants of crystal plasticity finite element models with different assumptions; the better one used an evolving yield surface based upon texture evolution.

RECOVERY AND RECRYSTALLIZATION

In both deformation processing to make sheet, and in forming of the cavity, heat treatments are required to restore ductility during deformation processing, or to drive out hydrogen or modify the interior surface of the cavity. These processes remove dislocations generated by plastic deformation, but this process is extremely sensitive to details of deformation history, preferred grain orientations, microstructure / grain size, heating rate, temperature, and time, making this process challenging to control. Compared to steels, niobium recrystallizes in a more random manner [17], making preferred textures more difficult to obtain. Having fewer processing variables available (compared to steel) also limits the ways that recrystallization can be used strategically to obtain desirable grain orientations.

Heat treating causes changes in the microstructure by recovery, recrystallization, and grain growth. These processes are briefly described using Figures 11 and 12 [18]. During plastic deformation, entangled dislocations cause dislocation multiplication processes [2-4]. Dislocation generation is a mechanism by which an intact plane of atoms is separated to become two terminated half-planes of opposite sign. Neighboring half planes with opposite signs have attractive stress fields that facilitate their joining together to make a full plane (Figure 11a). With thermal activation (heating), and diffusion, most of these terminated half planes are able to find neighboring half planes with the opposite sign, and join to recover a whole plane, which removes two dislocations (i.e., recovery). Such dislocation reactions eliminate *statistically stored dislocations*, and remaining *geometrically necessary dislocations* (which cause lattice curvature, Figure 11b) reorganize to form mobile low energy, low angle subgrain boundaries, Figure 11c.

Recrystallization and grain growth occur at higher temperatures than recovery, and follows partial recovery events. The recrystallization temperature depends on many factors, such as strain history, rate of heating (full recovery can prevent recrystallization) and purity. Impurities segregate preferentially to grain boundaries, and can stabilize boundaries and dislocation structures, so a higher temperature is needed to facilitate their motion.

There are many kinds of recrystallization [18]; the driving force for *primary* recrystallization is to reduce dislocation density by motion of grain boundaries. Figure 12a shows where subgrains that formed in a shear band are able to grow into lesser deformed adjacent material. Figure 12b illustrates a different scenario, where the smaller subgrain size in one grain has higher defect density, so the neighboring grain boundary bulges into this grain. As a grain boundary moves through a region with subgrains, atoms from grains with subgrains jump into perfect lattice sites, resulting in elimination of subgrains and most dislocations (there are always some dislocations present to satisfy the need for entropy). Because the strain energy of dislocations is so small in Nb, the density of dislocations in recrystallized grains is likely to be greater than in steels or most other metals. As

boundaries move, grains become larger, and the same voxel may have several boundaries pass through it. It is of great technological value to control which grain boundaries move in order to obtain desirable recrystallized orientations.

WELDING

Welding is a necessary part of fabricating accelerator hardware, although there are methods to make weldless cavities with hydroforming or spinning processes [19]. In current processes, half cells are e-beam welded together. As welding progresses, solidification, recrystallization and recovery occur near the weld, dramatically altering the parent microstructure in the heat affected and fusion zones [20]. Figure 13a shows a polycrystal weld in undeformed material that was exposed to air prematurely, so that differential oxidation rates revealed the grain structure. The fastest oxidation rates occurred on grains with {111} plane normals. In contrast, deformed single crystals recrystallize in the heat affected zone (HAZ), but the fusion part of the weld is often a bicrystal with a boundary along its centerline (Figure 13b). Grains within the fusion zone of polycrystals are large, and of varied orientations (Figure 13a,c), giving the weld very different properties compared to the parent material. The HAZ adjacent to the fusion zone of the weld has a dramatic gradient of grain sizes, and the heating allows adsorbed interstitial atoms to diffuse beneath the surface, altering purity in complex ways. Adjacent to the weld, recrystallization and dramatic grain growth occur, and farther away, some grain growth and recovery occurs to varying extents. The large grain sizes leads to a slightly lower yield stress and much more non-uniform strain, with elongations about half to 2/3 of the parent material. As the welded pieces are in fixtures, cooling will cause thermal contraction, so localized strain occurs in the weld and HAZ preferentially. In instrumented cavity tests, hot spots have most often been found in the HAZ of the equator weld, making the weld a suspicious source of defects that degrade cavity performance [19].

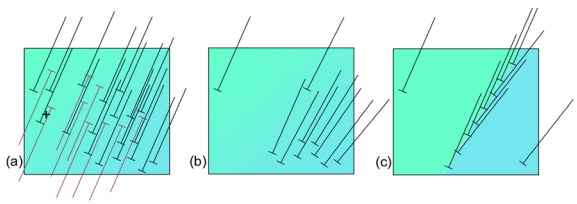

Figure 11: Schematic diagram of recovery; (a) after plastic deformation, statistically stored dislocations climb and glide to find annihilation partners (e.g. '+'), leaving only (b) geometrically necessary dislocations which (c) arrange themselves into low energy low angle boundaries.

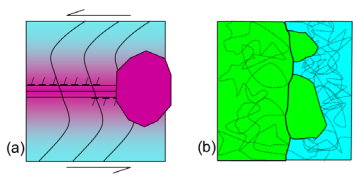

Figure 12: Schematic diagram of two forms of recrystallization; (a) subgrains within locally rotated shear bands nucleate to grow into surrounding lesser deformed material, (b) grain with larger subgrains (left) grow into grain with smaller subgrains (right).

SURFACE PREPARATION

After welding, the interior surface is chemically removed to eliminate a 'damaged layer' (about 100-200 μm) [19]. This damaged layer has been identified empirically, and it clearly removes any deformation features arising from handling, but it also removes {100} orientations that often predominate on the surface, which have a lower work function. An 800 °C vacuum heat treatment is often used to drive out hydrogen, and this causes a mixture of recovery and recrystallization that depends on the strain and location with respect to welds, so dislocation density is clearly reduced, but not in a uniform manner. While grain boundaries have been shown to trap vortices that cause local heating [5-7], it is not clear if dislocation substructure is also able to do this. Correlations between hot spots in cavities and higher geometrically necessary dislocation content have been identified in the context of experiments regarding the final 120 °C bake that improves performance. There are also correlations between hot spots and etch pits, which are often indications of dislocations, in the HAZ [21]. The role of dislocation rearrangement during the 120°C bake remains an open question.

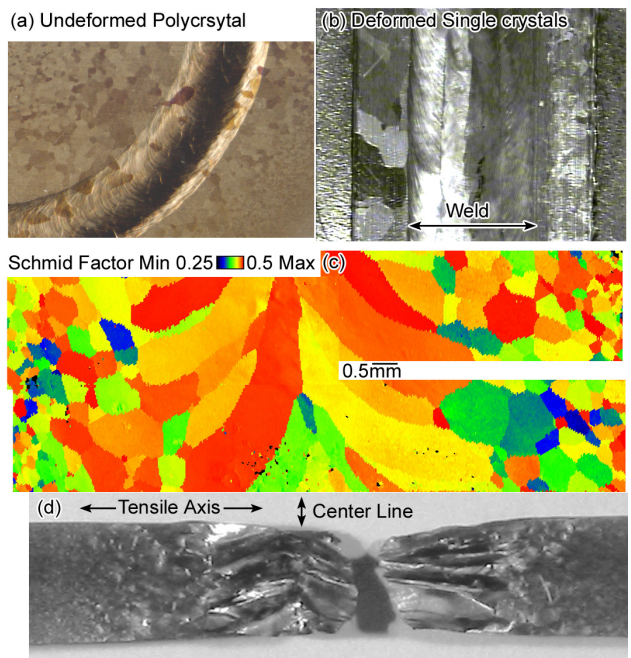

Figure 13 (a) Test weld on an undeformed polycrystal plate exposed to air while cooling shows differential oxidation that reveals the microstructure present in the material. (b) Weld between two deformed single crystals has a single orientation on either side in the fusion zone, but recrystallization occurs in the HAZ. Grains with high Schmid factors from OIM map (c) deform preferentially during a tensile experiment (d).

DISLOCATION SUBSTRUCTURE AND THERMAL PROPERTIES

Thermal conductivity (k) is also sensitive to dislocation content. Nonsuperconducting electrons conduct heat, but their fraction decreases with temperature, as does k. Lattice defects interfere with normal electron conduction, a component of k, but dislocations can also affect phonon transport [22]. A common way to semi-quantitatively assess dislocation density is with electrical resistivity [2]. High Q values have been obtained because the high purity increases k by removing heterogeneous sites that disturb electron flow. When unpinned segments of dislocations are aligned with the heat flow direction, a passing phonon can be dissipated by causing the dislocation to vibrate within its energy well, and thus reduce energy transport to the surrounding He bath. Figure 14 shows how k depends on RRR value (which may reflect both purity *and* dislocation content), and how a heat treatment of a deformed polycrystal specimen in a low purity environment degraded thermal conductivity above 3 K, but restored the phonon peak below 3 K. In recent bi-crystal experiments, differences in k with respect to crystal orientation as well as resistance at a grain boundary are resolved, though these effects are smaller than effects due to purity or dislocation content.

SUMMARY

This overview of the mechanical and physical metallurgy associated with the production of SRF cavities clearly shows that dislocations are an omnipresent facilitator for and detractor of the performance of cavities. There is only a small amount of knowledge about the underlying physics of dislocations on functional performance. Processing paths can be optimized to obtain desirable microstructures for forming, but there is also evidence that dislocations affect thermal conductivity and RF currents on the interior surface. Two exemplary forming histories illustrate where deeper understanding of the metallurgical state is needed: One can save cost by slicing ingots, but it is also likely to bring variability arising from large crystal orientations and welds. Cost savings may also be possible if strategic deformation processing is used to optimize Nb for hydroforming in order to remove the variability of welds [24]. Perhaps a recrystallized single-crystal or large grain cavity with few dislocations aligned with the direction of heat flow may lead to optimal and reproducible performance of a cavity. Whether this can be done without compromising other practical design constraints (such as strength or dimensional stability) presents an optimization challenge.

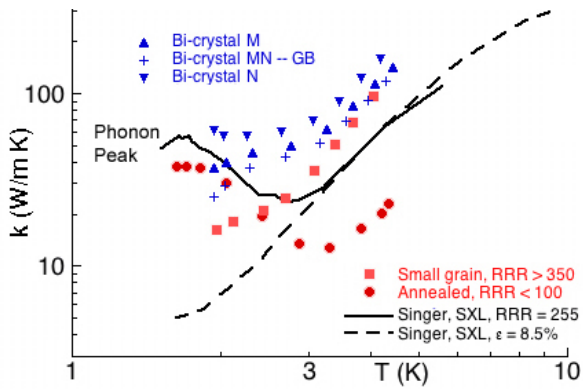

Figure 14: Measurement of thermal conductivity, k: the two curves from Singer [23] show how strain in a single crystal removes the phonon peak. An as-received polycrystal (orange symbols) showed no phonon peak, but after a 1400°C anneal, the phonon peak returned, but due to a low quality vacuum, the thermal conductivity at higher T dropped extensively. A bi-crystal specimen (blue symbols) shows modest effects of grain orientation and boundary on k.

REFERENCES

[1] G. Ciovati, J. Appl. Phys. 96(3) (2004), 1591.
[2] R. Abbaschian, L. Abbaschian, R.E. Reed-Hill, Physical Metallurgy Principles 4th ed. , PWS-Kent, Cengage Learning, 2009.
[3] D. Hull and D.J. Bacon, Introduction to Dislocations, 4th ed. Butterworth-Heinemann, 2001.
[4] G.E. Dieter, Mechanical Metallurgy, 3rd ed., McGraw-Hill Science Engineering, 1986.
[5] A. Romenenko, Ph.D. Dissertation, Cornell University, 2009.
[6] A. Gurevich, Appl. Phys. Lett. 88, 012511 (2006)
[7] G. Ciovati, A. Gurevich, Phys. Rev. Special Topics-Accelerators and Beams 11(12) 122001 (2008).
[8] G. Simmons, H. Wang, Single Crystal Elastic Constants and Calculated Aggregated Properties: A handbook, 2nd ed. MIT Press, Cambridge, MA (1971).
[9] D. Baars, T. Bieler, P. Darbandi, F. Pourboghrat, C. Compton, SRF 2009, Berlin, Sept. 21-25, TUOBAU05.
[10] A. Seeger, U. Holzwarth, Phil Mag, 86 (2006) 3861.
[11] R. Groger, A.G. Bailey, V. Vitek, Acta Mater. 56, (2008), 5401.
[12] D. Baars, T.R. Bieler, A. Zamiri, F. Pourboghrat, C. Compton, SRF 2007 Beijing, China, Oct. 14-19, TUP05, http://web5.pku.edu.cn/srf2007/.
[13] P. Kneisel, G. R. Myneni, G. Ciovati, J. Sekutowicz, T. Carneiro, AIP Conf. Proc. Aug. 9, 2007 Vol 927, (2007) 84.
[14] D. Raabe, K. Lucke, Z. Metallkunde, 85(5) (1994) 302.
[15] K.T. Hartwig, J. Wang, D.C. Baars, T.R. Bieler, S.N. Mathaudhu, R.E. Barber, IEEE Trans. Appl. Superconductivity 17(2), (2007), 1305.
[16] A. Zamiri, H. Jiang, T.R. Bieler, and F. Pourboghrat, JOM 59(7) (2008) 70.
[17] D. Baars, H. Jiang, T.R. Bieler, A. Zamiri, F. Pourboghrat, and C. Compton, Ceramic Trans. 201, (2008) 391.
[18] R.D. Doherty, D.A. Hughes, F.J. Humphreys, J.J. Jonas, D. Juul Jensen, M.E. Kassner, W.E. King, T.R. McNelley, H.J. McQueen, A.D. Rollet, Mater. Sci. Eng. A238 (1997) 219.
[19] H. Padamsee, J. Knobloch, T. Hays, RF Superconductivity for Accelerators, 2nd ed., Wiley-VCH, 2008.
[20] H. Jiang, T.R. Bieler, C. Compton, T. Grimm, PAC 2003 (12-19 May, Portland Oregon), IEEE Publishing, (2003), pp. 1359-1361.
[21] X. Zhao, G. Ciovati, C.E. Reece, A.T. Wu, SRF 2009, Berlin, Sept. 21-25, TUPPO087.
[22] E.F. Cotts, D.M. Miliotis, A.C. Anderson, Phys. Rev. B 24:12 (1981) 7336.
[23] W. Singer, A. Brinkmann, A. Ermakov, J. Iversen, G. Kreps, A. Matheisen, D. Proch, D. Reschke, X. Singer, M. Spiwek, H. Wen, H.-G. Brokmeier, LINAC 2006, Knoxville, TN, Aug 21-26, 2006.
[24] W. Singer, Physica C 441 (2006) 89–94.